

CHAMELEON: Foundation Models for Fairness-aware Multi-modal Data Augmentation to Enhance Coverage of Minorities

Mahdi Erfanian
University of Illinois Chicago
merfan2@uic.edu

H. V. Jagadish
University of Michigan
jag@umich.edu

Abolfazl Asudeh
University of Illinois Chicago
asudeh@uic.edu

ABSTRACT

The potential harms of the under-representation of minorities in training data, particularly in multi-modal settings, is a well-recognized concern. While there has been extensive effort in detecting such under-representation, resolution has remained a challenge.

With recent advancements in generative AI, large language models and foundation models have emerged as versatile tools across various domains. In this paper, we propose CHAMELEON, a system that efficiently utilizes these tools to augment a data set with a minimal addition of synthetically generated tuples, in order to enhance the coverage of the under-represented groups. Our system follows a rejection sampling approach to ensure the generated tuples have a high quality and follow the underlying distribution. In order to minimize the rejection chance of the generated tuples, we propose multiple strategies for providing a guide for the foundation model. Our experiment results, in addition to confirming the efficiency of our proposed algorithms, illustrate the effectiveness of our approach, as the unfairness of the model in a downstream task significantly dropped after data repair using CHAMELEON.

PVLDB Reference Format:

Mahdi Erfanian, H. V. Jagadish, and Abolfazl Asudeh. CHAMELEON: Foundation Models for Fairness-aware Multi-modal Data Augmentation to Enhance Coverage of Minorities. PVLDB, 14(1): XXX-XXX, 2020. doi:XX.XX/XXX.XX

PVLDB Artifact Availability:

The source code, data, and/or other artifacts have been made available at <https://github.com/UIC-InDeXLab/Chameleon>.

1 INTRODUCTION

“The CHAMELEON changes color to match the earth, the earth doesn’t change color to match the chameleon.” – SENEGALESE PROVERB

With the wide use of machine learning, the importance of using appropriate data sets is now well-recognized. In particular, there is increasing awareness of unfairness towards minorities and other marginalized groups on account of their under-representation in the training data. There is now a growing body of work on *coverage* in a training data set [5, 48, 62], giving us tools to detect such under-representation.

Of course, detecting under-representation does not in itself address the problem: we then need to fix it somehow, for example by

integrating data from external sources [50]. If additional data could be collected, that would be ideal, but this is frequently not possible. An approach in such cases is to generate synthetic data. Indeed, such approaches have been explored for regular alphanumeric data, such as in relational tables [16, 19, 27, 32].

Multi-modal data is increasingly being used for analysis, exploiting huge recent advances in technologies such as image recognition. In fact, bias in multi-modal training data has been noticed for quite some time, beginning with the well-know case of early google software labeling an African American woman as a gorilla [49], and continuing through many other cases [15, 38, 56, 65]. This begs the question, what can we do once we have detected that a multi-modal dataset is biased, with insufficient representation of certain groups? There is no obvious way we can apply techniques developed for alphanumeric relational data.

This is the problem we tackle in this paper. Our central idea is to use generative AI to create synthetic data for this purpose. While this idea has immediate appeal, particularly given the spectacular recent advances in Foundation Models, actually getting it to work requires overcoming many challenges. First, we have to determine the minimal set of synthetic tuples that once added to the original data set, under-representation issues are resolved. Second, in order to prevent a distribution shifts due to synthetically generated tuples, we need to ensure that the generated data follows the underlying distribution represented by the input data set. Third, we have to ensure the generated images are actually reasonable and have a high quality to look realistic to a human evaluator. Last but not least, given the (often monetary) cost associated with the queries to the foundation model, we should ensure the cost-effectiveness of the data set repair process.

To address the first challenge, using the notion of data coverage [5, 62] for identifying under-representation, we formally define the COMBINATION-SELECTION problem, which minimizes the total number of synthetic tuples for resolving lack of coverage of minorities at the most general level. We show the problem is NP-hard, and propose a greedy approximation algorithm for it. For the second challenge, we view each tuple in the data set \mathcal{D} as an independent and identically distributed (iid) random sample from the underlying distribution ξ it represents. We use the vector representations (embeddings) space to describe the distribution. Then, a newly generated tuple is discarded if it fails the data distribution test, i.e., if it is unlikely to be generated by ξ . To address the third challenge, we model the quality evaluation as hypothesis testing, and reject the samples that have a higher chance of being labeled as “unrealistic” by a random human evaluator. Finally, to minimize the number of queries to the foundation model, we provide a guide tuple (and a mask), in addition to the prompt, to the foundation model. We

This work is licensed under the Creative Commons BY-NC-ND 4.0 International License. Visit <https://creativecommons.org/licenses/by-nc-nd/4.0/> to view a copy of this license. For any use beyond those covered by this license, obtain permission by emailing info@vldb.org. Copyright is held by the owner/author(s). Publication rights licensed to the VLDB Endowment.

Proceedings of the VLDB Endowment, Vol. 14, No. 1 ISSN 2150-8097. doi:XX.XX/XXX.XX

propose multiple strategies for guide selection such that the chance of passing the distribution and the quality tests is maximized.

Summary of contributions. We introduce CHAMELEON, a system that uses foundation models to augment multi-modal data sets in order to enhance their representation of the minorities, in form of data coverage. To the best of our knowledge, our paper is *the first to use foundation models for fairness-aware data augmentation*. In summary, our contributions are the following:

- We propose fairness-aware data augmentation using foundation models for resolving lack of coverage in multi-modal data (§ 2).
- Following a rejection sampling approach, we propose data distribution and quality evaluation tests to ensure the augmented tuples do not deviate from the underlying data distribution, and have as high quality as the real tuples in the data set (§ 3).
- We propose the COMBINATION-SELECTION problem, which specifies the description of the tuples to be generated with the goal to resolve lack of coverage with minimum amount of augmentation to the data set. We prove that the COMBINATION-SELECTION problem is NP-hard, and propose a greedy approximation algorithm with the logarithmic approximation-ratio for it (§ 4).
- We propose the Guide-selection problem that provides a guide tuple and a mask as the input to the foundation model in order to maximize the chance of passing the rejection sampling tests. We propose multiple strategies for guide-selection, including a solution based on contextual multi-armed bandit (§ 5).
- We conduct comprehensive experiments on real and synthetic data sets to evaluate the efficiency of the proposed algorithms in comparison to the baselines and to study their effectiveness using human evaluators. We also provide an experiment that illustrates the unfairness (performance disparity) of a CNN model on uncovered groups significantly decreases when trained on a repaired data set using CHAMELEON (§ 6).

2 PRELIMINARIES

2.1 (Input) Data Model

We are given a data set of multi-modal tuples (e.g., images) $\mathcal{D} = \{t_1, \dots, t_n\}$, as a collection of independent and identically distributed (iid) samples, taken from an (unknown) distribution ξ . The tuples are associated with $d \geq 1$ attributes of interest $\mathbf{x} = \{x_1, \dots, x_d\}$ (e.g., gender, race, age-group, etc.), that are used for identifying (demographic) groups. Without loss of generality, we assume the attributes of interest are categorical (we assume the continuous attributes are properly bucketized). Attributes of interest can be unordered (e.g., gender and race) or ordinal (e.g., age-group). Each attribute has a cardinality of two or more. For example, an attribute sex (biological sex) with values {male, female} partitions the individuals into two non-overlapping groups. We use $dom(x_i)$ to represent the domain of the attribute $x_i \in \mathbf{x}$, i.e., the set of valid values for x_i .

The cartesian product of values on a subset of attributes $\mathbf{x}' \subseteq \mathbf{x}$, form a set of (demographic) subgroups. For example, {white male, white female, black male, ...} are the subgroups defined on the attributes (race, gender). We refer to the number of attributes used to specify a subgroup as the *level* of that subgroup. For example, the level of the subgroup white male is 2, while the level of the subgroup

Table 1: Table of Notations

Notation	Description
$\mathcal{D} = \{t_1 \dots, t_n\}$	the data set
$\mathbf{x} = \{x_1 \dots, x_d\}$	attributes of interest
$dom(x_i)$	the set of valid values for the attribute x_i
$\ell(\mathbf{g})$	the level of a subgroup \mathbf{g}
τ	the coverage threshold
P_i	a pattern, specifying a subgroup over \mathbf{x}
c_i	a combination in $\times_{k=1}^d dom(x_k)$
\mathcal{F}	the foundation model
v	the query cost of <i>FM</i>
ξ	the underlying distribution of \mathcal{D}
$\vec{v}(t_i)$	the vector representation of t_i

male is 1. We use $\ell(\mathbf{g})$, to refer to the level of a subgroup \mathbf{g} . Similarly, we say a subgroup \mathbf{g}' is a subset of \mathbf{g} , if the groups specifying \mathbf{g}' are a superset of the ones for \mathbf{g} . For example {white male preschooler} is a subset of the more general group {white male}. That is, the set of individuals in group {white male preschooler} are a subset of {white male}. Moreover, we say a subgroup \mathbf{g} is a *parent* of the subgroup \mathbf{g}' , if $\mathbf{g}' \subset \mathbf{g}$ and $\ell(\mathbf{g}) = \ell(\mathbf{g}') + 1$. For example, the subgroup {white male} is a parent of the subgroup {white male preschooler}. Finally, slightly abusing the terms, we call a subgroup a *combination* if $\ell(\mathbf{g}) = d$. Furthermore, we say two combinations are “sibling” if they differ in exactly one attribute (with their values the same on all other attributes).

2.2 (Input) Foundation Model

We assume access to a foundation model \mathcal{F} (e.g., DALL-E 2¹) for data generation. In the following, we discuss the requirements relevant to this project. We treat \mathcal{F} as black-box, which allows the adaptation of both closed-source and open-source foundation models. For more information about the foundation models, please refer to [11, 14, 76]. We consider the foundation model \mathcal{F} with the following inputs that generates a synthesized output tuple:

- **Prompt:** a natural language description of an instruction that specifies the details of the tuple to be generated. For example, a prompt for image generation could be “A realistic photo of a white cat”.
- **Guide:** when only provided with a prompt, the foundation model uses its “imagination” to generate the requested tuple. For example, for the previous cat-image example prompt, the breed and size of the cat, the background, and other details are chosen by the foundation model. Alternatively, a guide can be provided to \mathcal{F} to influence the generation process. We formalize the guide as a pair (t, m) , where t is a tuple, and m is a mask. The mask m specifies which parts of the guide tuple should change. Continuing with the cat example, t can be a cat image and m can specify the foreground to be regenerated.

Cost model: We assume each query to the foundation model has a fixed cost v . The cost is monetary when using external foundation

¹CHAMELEON uses DALL-E 2 as its default image generator. “DALL-E 2 is an AI system that can create realistic images and art from a description in natural language.” <https://openai.com/dall-e-2>

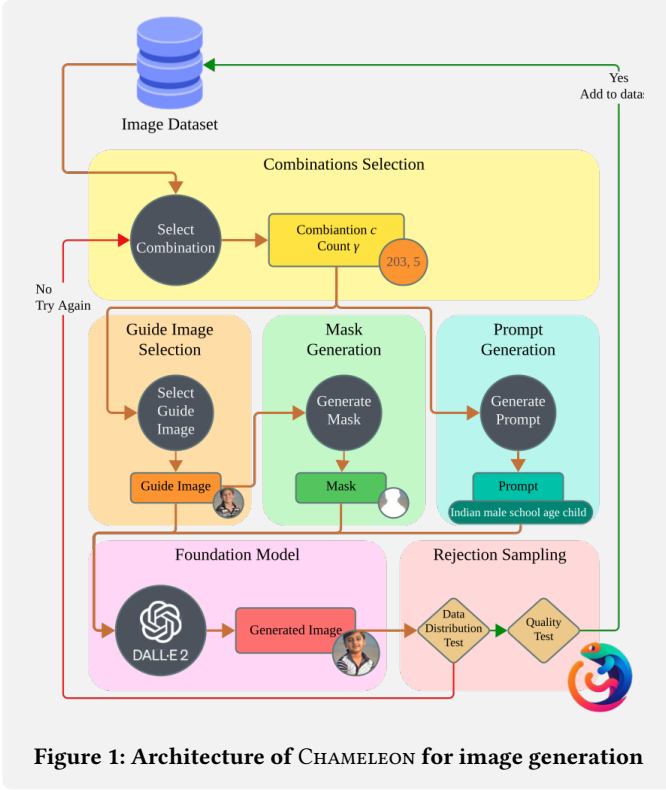


Figure 1: Architecture of CHAMELEON for image generation

models such as DALL-E 2, and it can be computational when the model is hosted locally.

2.3 (Objective) Data Coverage

We use the notion of *data coverage* [5] to identify lack of representation issues in a dataset \mathcal{D} . In particular, given a data set \mathcal{D} and a coverage threshold τ (e.g., $\tau = 50$), we say a subgroup g is *uncovered*, if $|g \cap \mathcal{D}| < \tau$. That is, the number of samples in \mathcal{D} from the group g are less than τ . When studying lack of coverage in a data set, we are usually interested in finding the most-general uncovered subgroups. That is, the collection of subgroups g such that (a) g is uncovered and (b) all parents of g are covered.

Following the notation in [5], we use *patterns* to refer to uncovered subgroups. A pattern P is a string of d values, where $P[i]$ is either a value from the domain of x_i , or it is “unspecified”, specified with X . For example, consider a dataset with three binary attributes of interest $\mathbf{x} = \{x_1, x_2, x_3\}$. The pattern $P = X01$ specifies all the tuples for which $x_2 = 0$ and $x_3 = 1$ (x_1 can have any value). The set of patterns that identify most-general uncovered subgroups are called *Maximal Uncovered Patterns* (MUPs). The level of a MUP is the same as the level of the subgroup it represents.

2.4 System Architecture Overview

Figure 1 shows the overall architecture of the system, whose components we will design in the rest of this paper. The augmentation process for a data set \mathcal{D} starts with specifying a small set of synthetic tuples (a set of combinations, each with a count) that once

generated and added to \mathcal{D} , resolve problematic lack of coverage issues (§ 4). Then for each combination, an input query is constructed to be passed to the foundation model. At minimum, this query comprises a text prompt describing the desired combination. However, that leaves too much latitude to the foundation model, and the result is likely to be an image unsuitable for the data set at hand (that is, it would be unlikely to occur in the underlying distribution of \mathcal{D}), even if it satisfies the prompt conditions. To avoid this, a guide tuple, and mask, is specified, in addition to the prompt (§ 5). The foundation model then generates a new tuple based on this input. Even with the augmented query, the produced tuple may not be satisfactory. We follow a rejection sampling strategy: the new tuple should pass a data distribution test and a quality test before it can be added to the dataset (§ 3).

3 REJECTION SAMPLING

Our strategy for ensuring the high quality of the augmented dataset is inspired by rejection sampling [29, 31]. In order to generate a sample from a distribution with the probability density function (pdf) f , the rejection sampling technique generates sample points under an upper-envelope of f and rejects it if the sample point does not fall under f . We follow a similar strategy. Specifically, when a new tuple is generated by the foundation model, we only accept it if it passes the data distribution test (§ 3.1) and the quality evaluation (§ 3.2). Otherwise, the generated tuple is rejected and we try again.

3.1 Data distribution test

When augmenting a data set, it is critical to ensure that added tuples follow the underlying data distribution ξ . For example, when the data set comprises wide-shot images at an office workplace the generated tuples should also belong to the same context. The first issue though is that ξ is unknown. Besides, it is not clear how to quantify and represent the distribution, while relying on the foundation model’s imagination could cause a distribution drift.

We utilize the vector representation (aka embedding) of the tuples for representing the distribution ξ . Given a tuple t_i , let $\vec{v}(t_i) = \vec{v}_i = \langle v_1, v_2, \dots, v_k \rangle$ be its embedding. We assume the embeddings are accurate. That is, the cosine similarity between the embeddings represent the semantic similarity between two tuples. Formally, the similarity of two tuples t_i and t_j can be computed as $\mathcal{S}_{im}(t_i, t_j) = \cos \angle(\vec{v}_i, \vec{v}_j)$. Now, in the embedding space let ξ be the probability distribution from which \mathcal{D} is sampled. Hence, the probability that a tuple t is sampled is $Pr_{\xi}(t)$. We use $\vec{\mu}_{\xi}$ to represent the mean of ξ . Since the tuples in \mathcal{D} are iid samples from ξ , those can be used for estimating $\vec{\mu}_{\xi}$. Let \vec{v}_c be the sample mean of the representation vectors in \mathcal{D} . That is, $\vec{v}_c = \frac{1}{m} \sum_{t_i \in \mathcal{D}} \vec{v}_i$. Assuming that n (the size of \mathcal{D}) is large enough, based on the central limit theorem we can estimate $\vec{\mu}_{\xi}$ as \vec{v}_c .

To ensure that generated tuples adhere to the underlying distribution ξ , we employ a one-class support vector machine (OCSVM) approach proposed by Scholkopf et al. [59] as a quality control mechanism.

Formally, given a set of training embeddings $\{\vec{v}_1, \vec{v}_2, \dots, \vec{v}_n\}$ representing tuples drawn from ξ , the OCSVM aims to learn a decision boundary that separates the majority of these embeddings from the origin in the feature space. This boundary implicitly defines a

region that characterizes the "normal" or acceptable embeddings. To find this boundary (hyperplane), the following optimization problem is proposed:

$$\min_{\mathbf{w}, \rho, \epsilon} \frac{1}{2} \|\mathbf{w}\|^2 + \frac{1}{\nu n} \sum_{i=1}^n \epsilon_i - \rho$$

$$\text{Subject to } \mathbf{w} \cdot \phi(\vec{v}_i) \geq \rho - \epsilon_i, \quad \epsilon_i \geq 0, \quad i = 1, 2, \dots, n$$

where:

- \mathbf{w} is the hyperplane normal vector (weight vector)
- ν is an upper-bound on the fraction of outliers and a lower bound on the fraction of support vectors (SV)
- ϕ is a feature mapping function that maps embeddings into a higher-dimensional space (e.g., the radial basis function kernel)
- ρ is a parameter controlling the margin of the decision boundary
- ϵ_i are slack variables allowing for a soft margin

To evaluate a generated tuple t_g with embedding \vec{v}_g , we project it into the feature space using the kernel function and compute:

$$f(\vec{v}_g) = \mathbf{w} \cdot \phi(\vec{v}_g) - \rho$$

If $f(\vec{v}_g) \geq 0$, the tuple is deemed acceptable, falling within the normal region defined by the OCSVM. If $f(\vec{v}_g) < 0$, it is potentially deviating from the desired distribution and is rejected.

3.2 Quality evaluation

Foundation models have become strong tools for creating high quality multi-modal data. Still, due to the randomized nature of their generation process, as well as the task-specific difficulties of various queries, some of the generated tuples may not look *realistic to human beings*.

We note that our evaluation of the generated tuples is qualitative and subjective. That is, the answer to "does this tuple look realistic" may vary from one person to the other. However, if there is good correlation between raters, *the probability* of the answer being positive reflects the quality of the tuple.

Using this observation, we model the quality of a tuple as a *Bernoulli random variable*. Specifically, let p be the probability that a human evaluator labels a randomly sampled (real) tuple from the distribution ξ as "realistic". In other words, with probability $(1-p)$ the evaluator will mistakenly labels the tuple as "unrealistic". We can then define the Bernoulli variable ϕ , which is one if a real tuple labeled as realistic by a human evaluator, and zero otherwise. Therefore, the pdf of ϕ for the randomly sampled (real) tuples is,

$$f(\phi) = \begin{cases} p & \phi = 1 \\ (1-p) & \phi = 0 \end{cases} \quad (1)$$

The mean and the variance of this Bernoulli distribution are $\mu_\phi = p$ and $\sigma_\phi^2 = p(1-p)$, respectively.

Let p' be the probability that a randomly selected human evaluator labels a AI-generated tuple as realistic. When the generated tuple is unrealistic $p' < p$, otherwise the human-evaluator is not better than random labeling. We use this observation and develop a hypothesis testing. Particularly, we discard an AI-generated tuple, if we can reject the null hypothesis that p' is equal to p , i.e., $\mathcal{H}_{null} : p' = p$. Then, considering the lower tail test, the alternative hypothesis would be $\mathcal{H}_{alt} : p' < p$.

To do so, we first obtain a sufficiently large sample set U of evaluations, where each sample is drawn using a randomly selected

evaluator and a random (real) tuple from \mathcal{D} . Let m_U be the sample mean of U . Since U is sufficiently large, we can estimate $p = \mu_\phi$ with m_U . Now for a generated tuple t , consider a sample set U_t of N evaluations of t , each using a randomly selected evaluator. We assume a (small) fixed-size budget for each generated tuple. Let m_t and s_t be the sample mean and the standard deviation for U_t . Since N is small, we use the Student's t-test. Specifically,

$$t_{N-1} = \frac{m_t - p}{s_t / \sqrt{N}}$$

Next, using the t-table, we obtain the left sided p-value and evaluate its significance level. If the p-value is smaller than a significance goal α , we reject the null hypothesis (discard the generated tuple).

4 COMBINATION SELECTION

Our overall goal is to use the foundation model and generate a minimal set of synthetic tuples to resolve the problematic MUPs (with the smallest levels). Therefore, we consider an iterative approach, where during each iteration we resolve the MUPs at the smallest level. Given a data set \mathcal{D} , let \mathcal{M} be the set of MUPs, and let \mathcal{M}^* be the set of MUPs with the minimum level. That is $\mathcal{M}^* = \{M \in \mathcal{M} \mid \ell(M) = \min_{M' \in \mathcal{M}} (\ell(M'))\}$. For each MUP $M \in \mathcal{M}^*$, let us define its gap $\delta(M) = \tau - |\mathcal{D} \cap M|$; i.e., the coverage threshold minus the current coverage of M in \mathcal{D} . In other words, $\delta(M)$ is the minimum number of synthetic tuples matching M we need to obtain before it is covered. Also, for each combination $c_i \in \times_{k=1}^d \text{dom}(x_k)$, let σ_i be the number of synthetic tuples from that combination. Then, the "COMBINATION-SELECTION" problem is to assign the values of $\sigma_i > 0$ such that (i) for each MUP $M \in \mathcal{M}^*$, at least $\delta(M)$ generated tuples match it, and (ii) sum of all σ_i values is minimized. Formally,

$$\begin{aligned} \min & \sum_{c_i} \sigma_i \\ \text{Subject to} & \sum_{c_i \in \text{match}(M)} \sigma_i \geq \delta(M), \quad \forall M \in \mathcal{M}^* \end{aligned}$$

LEMMA 1. COMBINATION-SELECTION is NP-hard.²

Since COMBINATION-SELECTION is NP-hard, we design an approximation algorithm for this step. Our algorithm follows the *greedy* scheme. Algorithm 1 shows the pseudo-code of the GREEDY algorithm. The algorithm is iterative, where at each iteration it finds the combination that matches the maximum number of remaining MUPs in \mathcal{M}^* . We utilize the inverted index and the tree data structure proposed in [5] for finding c . The algorithm then finds the minimum gap γ in the MUPs matching c and increases the number of instances from c by γ . It also updates the gaps for the MUPs matching c and remove the ones that reach to a gap of zero from \mathcal{M}^* .

THEOREM 1. *The approximation ratio of the GREEDY approach is $\log(\eta)$, where $\eta = \sum_{M \in \mathcal{M}^*} \delta(M)$.*

5 GUIDE TUPLE SELECTION

Given a combination c , we would like to generate a tuple that matches c and is likely to pass the rejection sampling tests. Therefore, we want to make sure that (a) the generated tuple follows the

²Proofs are provided in § 8.

Algorithm 1 GREEDY

Input: The smallest-level MUPs \mathcal{M}^* **Output:** The number of instances from each combination to be augmented to \mathcal{D}

```
1:  $\sigma \leftarrow \text{new hashmap}()$ 
2: for  $M \in \mathcal{M}^*$  do
3:    $\delta(M) \leftarrow \tau - |\mathcal{D} \cap M|$ 
4: while  $\mathcal{M}^*$  is not empty do
5:   find the combination  $c$  that matches most MUPs in  $\mathcal{M}^*$ 
6:    $\mathcal{M}' \leftarrow \{M \in \mathcal{M}^* \mid c \text{ matches } M\}$ 
7:    $\gamma \leftarrow \min_{M \in \mathcal{M}'} \delta(M)$ 
8:   if  $c \in \sigma.\text{keys}$  then
9:      $\sigma[c] \leftarrow \sigma[c] + \gamma$ 
10:  else  $\sigma[c] \leftarrow \gamma$ 
11:  for  $M \in \mathcal{M}'$  do
12:     $\delta(M) \leftarrow \delta(M) - \gamma$ 
13:    if  $\delta(M) = 0$  then
14:      Remove  $M$  from  $\mathcal{M}^*$ 
15: return  $\sigma$ 
```

underlying distribution ξ represented by \mathcal{D} and (b) the generated tuple has a high quality and passes the quality evaluation. So, instead of relying on the foundation models imagination, we provide a “guide” for the generation process. Recall from § 2.2, that the guide is a pair (t, m) , where t is a tuple and m is a mask. In the following, we propose various strategies for guide tuple selection. We begin with a baseline approach discussed in § 5.1 and progressively explore more sophisticated strategies in § 5.2 and § 5.3.

In the context of images, a mask specifies the parts of the guide image that should be regenerated. Our mask generation (§ 5.4) involve cropping the foreground of t using a mask m , ensuring that the foundation model regenerates only the portions delineated by the mask m .

5.1 Random-Guide Strategy

The random guide strategy focuses on the first requirement that: the generated tuple should follow the underlying distribution ξ , represented by \mathcal{D} . Then, viewing each tuple t as a random sample from \mathcal{D} , it selects the guide tuple uniformly at random from the data set without taking into account the target combination c . While the random-guide strategy is appropriate for satisfying the underlying distribution, it ignores the second requirement of passing the quality test. We experimentally show in § 6, that tuples generated based on this strategy have a lower chance of passing quality evaluation.

5.2 Similar-Tuple Strategy

The similar-tuple strategy creates a pool of similar combinations to the target combination c . Combinations c_1 and c_2 are considered *similar* if (a) they are *siblings* (i.e., their values differ in exactly one attribute) and (b) one of the following conditions is satisfied. Let d_i be the attribute on which c_1 and c_2 differ. If d_i is non-ordinal then c_1 and c_2 are considered similar. However, if d_i is ordinal, then the distance between c_1 and c_2 should be 1 to be considered similar. Formally, for two sibling combinations c_1 and c_2 that differ in attribute d_i :

$$\text{similar}(c_1, c_2) = \begin{cases} \text{false} & \text{if } d_i \text{ is ordinal and } |c_1[d_i] - c_2[d_i]| > 1 \\ \text{true} & \text{otherwise} \end{cases}$$

Subsequently, it selects a guide tuple from the pool of similar combinations, assigning weights to each element based on the number of tuples in \mathcal{D} that adhere to that particular combination. Formally, the pool of similar combinations can be defined as follows:

$$S = \left\{ c \in \text{sibling}(c_i) \mid \text{similar}(c_i, c) = \text{true} \right\}$$

For each combination $c_i \in S$, let $|c_i|$ be the number of tuples in \mathcal{D} matching it. That is, $|c_i| = |\mathcal{D} \cap c_i|$. We assign the sampling weight of each combination proportional to their normalized size:

$$w_i = \frac{|c_i|}{\sum_{c_j \in S} |c_j|}, \forall c_i \in S$$

The similar-tuple strategy then selects a combinations $c_i \in S$, randomly with probability w_i . It then returns random sample from the pool tuples in \mathcal{D} that match c_i , as the guide tuple. Using w_i as the weight ensures equal sampling probability for all tuples that match a combination in S .

This strategy considers tuples in the selection pool that closely resemble the target combination, differing in only one attribute of interest. It excludes tuples that are far away from the target combination. It also excludes the tuples with the exact combination as the target combination. This exclusion is intentional to deal with the fact that the target combination c is not very common in the data set. Since c is not well-represented, picking guide tuples from this group might make all the chosen tuples look too similar. By considering combinations that are similar but not exactly the same as the target one, the strategy aims to make sure we get a more varied and representative set of guide tuples for the generation process.

5.3 Modeling as Contextual Multi-armed Bandit

Our LINUCB strategy models the guide tuple selection problem as a *contextual multi-armed bandit* problem [12], and uses *Contextual Upper Confidence Bound* for solving it [40]. Specifically, it models each attribute as a bandit arm. Then given a target combination c , it selects an arm to pull (i.e., an attribute to modify), aiming to maximize the obtained reward. In each iteration, we have the opportunity to pull only one arm, signifying the ability to alter one attribute value within the target combination to a new value. The reward obtained from pulling that arm is then observed. The objective is to learn the optimal arm to pull for a given combination c over successive iterations.

To provide further clarification, let us discuss an example within the context of images. Consider a data set with attributes of interest including gender, race, and age-group. The foundation model \mathcal{F} may perform better in modifying the race of a subject compared to altering their age group for specific combinations (e.g., Asian female adults). However, its performance may vary for other combinations. LINUCB aims to systematically explore different arms to pull (e.g., changing race, gender, or age group) and exploit the arm yielding the highest reward over time.

Formally, we formulate the guide tuple selection problem as a contextual multi-armed bandit problem. We consider the attributes of interest, denoted as $\mathbf{x} = \{x_1, x_2, \dots, x_d\}$, as arms of the bandit $\mathbf{a} = \{a_1, a_2, \dots, a_d\}$. The *context*, AKA the *feature vector*, is then defined as a one-hot vector \mathbf{f} representing combinations, where 1

is assigned for the input combination c and 0 for all other elements. Let $k = |\times_{i=1}^d \text{dom}(x_i)|$ be the number of possible combinations. The size of the feature vector $\mathbf{f}_{s,a}$ is $(k \times 1)$ where s denotes the time step of the algorithm.

We define the reward function based on whether a generated tuple passes the rejection sampling tests. Let $\text{pass}()$ be a binary function that is false if a generated tuple is rejected. Then,

$$r_{s,a} = \begin{cases} 1 & \text{if } \text{pass}() = \text{true} \\ 0 & \text{otherwise} \end{cases}$$

We adopt ‘‘LinUCB with Disjoint Linear Models’’ [40] to balance exploration and exploitation. At every iteration s , for every arm $a \in \mathbf{a}$, given the context $\mathbf{f}_{s,a}$, LINUCB computes confidence intervals for the expected reward and selects the arm with the maximum upper bound of reward to be explored next.

We assume that the expected reward of an arm a is linear in its k -dimensional input context $\mathbf{f}_{s,a}$ with some unknown coefficient vector $\theta_{s,a}^*$, formally given by: $E[r_{s,a} | \mathbf{f}_{s,a}] = \mathbf{f}_{s,a}^\top \theta_{s,a}^*$

Assuming that m is the number of times arm a has been pulled so far ($s \geq m$), we define $\mathbf{F}_{s,a}$ with size $(m \times k)$ as the matrix consisting of all previously observed contexts for arm a .

$$\mathbf{F}_{s,a} = [\mathbf{f}_{1,a}^\top, \dots, \mathbf{f}_{m,a}^\top]^\top$$

We also have a vector of observed rewards from pulling arm a .

$$\Gamma_a = [r_{1,a}, \dots, r_{m,a}]^\top$$

Vector \mathbf{b}_a is defined as: $\mathbf{b}_a = \mathbf{F}_{s,a}^\top \Gamma_a$

Using Ridge regression estimator, we can estimate the coefficients of each arm a as:

$$\hat{\theta}_{s,a} = (\mathbf{F}_{s,a}^\top \mathbf{F}_{s,a} + \mathbf{I}_k)^{-1} \mathbf{b}_a$$

Thus, in each iteration s of the algorithm, we select arm a_s using:

$$a_s = \underset{a \in \mathbf{a}}{\text{argmax}} (\mathbf{f}_{s,a}^\top \hat{\theta}_{s,a} + \alpha \sqrt{\mathbf{f}_{s,a}^\top \mathbf{A}_a^{-1} \mathbf{f}_{s,a}})$$

where $\mathbf{A}_a = \mathbf{F}_{s,a}^\top \mathbf{F}_{s,a} + \mathbf{I}_k$ and α is a hyper-parameter to balance exploitation and exploration.

After pulling arm a_s in iteration s , we observe the reward $r_{s,a_s} \in \{0, 1\}$ where 1 indicates that the generated tuple t has passed quality and data distribution tests. We can update matrices \mathbf{A}_{a_s} and \mathbf{b}_{a_s} as:

$$\begin{aligned} \mathbf{A}_{a_s} &\leftarrow \mathbf{A}_{a_s} + \mathbf{f}_{s,a_s} \mathbf{f}_{s,a_s}^\top \\ \mathbf{b}_{a_s} &\leftarrow \mathbf{b}_{a_s} + r_{s,a_s} \mathbf{f}_{s,a_s} \end{aligned}$$

Algorithm 2 presents the pseudo-code for the LINUCB strategy used in selection of guide tuple t from the dataset \mathcal{D} .

5.4 Mask Delineation

In the context of images, once the guide tuple t is selected, we delineate the foreground subject using a mask. This mask serves as an indicator, specifying the regions to be cropped and regenerated from the tuple t . The delineation of the border around the subject can be achieved with different levels of precision. A precise border sketch preserves more space from the original context, potentially resulting in a higher acceptance rate for data distribution test. However, it may limit the foundation model imagination capacity and lead to lower acceptance rate for quality evaluation test. We propose three levels of mask sketch accuracy: *accurate*, *moderate*, and *imprecise* (Figure 2).

Algorithm 2 LINUCB

Input: Attributes of interest as arms $\mathbf{a} = \{a_1, \dots, a_d\}$, exploration parameter α , $k = |\times_{i=1}^d \text{dom}(x_i)|$

Output: Sequence of selected guide tuples and observed rewards

- 1: **for** $a \in \mathbf{a}$ **do**
- 2: $\mathbf{A}_a \leftarrow \mathbf{I}_k$, $\mathbf{b}_a \leftarrow \mathbf{0}_{k \times 1}$ ▷ Initialize matrices
- 3: **for** each iteration s **do**
- 4: $c_s \leftarrow \text{Input}()$ ▷ Get target combination
- 5: **for** $a \in \mathbf{a}$ **do**
- 6: $\hat{\mathbf{f}}_{s,a} \leftarrow \text{Convert}(c_s)$ ▷ Calculate context vector from c_s
- 7: $\hat{\theta}_{s,a} = \mathbf{A}_a^{-1} \mathbf{b}_a$ ▷ Estimate coefficients
- 8: $UCB_{s,a} = \hat{\mathbf{f}}_{s,a}^\top \hat{\theta}_{s,a} + \alpha \sqrt{\hat{\mathbf{f}}_{s,a}^\top \mathbf{A}_a^{-1} \hat{\mathbf{f}}_{s,a}}$ ▷ Calculate UCB
- 9: $a_s = \text{argmax}_{a \in \mathbf{a}} UCB_{s,a}$ ▷ Select arm a_s
- 10: $c' \leftarrow \text{Modify}(c, a_s)$ ▷ Modify attribute a_s of c to create new combination
- 11: $t \leftarrow \text{Select}(c')$ ▷ Select tuple t matching c'
- 12: $r_{s,a_s} \leftarrow \text{Input}()$ ▷ Observe reward for r_{s,a_s}
- 13: $\mathbf{A}_{a_s} \leftarrow \mathbf{A}_{a_s} + \mathbf{f}_{s,a_s} \mathbf{f}_{s,a_s}^\top$ ▷ Update matrices
- 14: $\mathbf{b}_{a_s} \leftarrow \mathbf{b}_{a_s} + r_{s,a_s} \mathbf{f}_{s,a_s}$

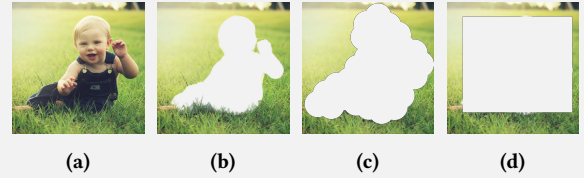


Figure 2: Illustration of various guide image (a) masks: (b) Accurate (c) Moderate (d) Imprecise mask

5.4.1 Accurate mask delineation. This represents the highest level of precision in mask delineation, achieved by utilizing the off-the-shelf background remover tool `rembg`.

5.4.2 Moderate mask delineation. To obtain a moderately delineated mask, we extend the border of the mask drawn in 5.4.1 by 10 percent of the image size. This extension is implemented using circles, with each point on the mask border being surrounded by a circle of radius equal to 10% of the image width.

5.4.3 Imprecise mask delineation. For an imprecise mask delineation, we expand the border of the mask drawn in 5.4.1 to form a rectangular area. This rectangle encompasses the previous mask, providing a less precise but more inclusive delineation.

6 EXPERIMENTS

This section presents results from experiments to evaluate the efficacy of our proposed system, CHAMELEON. We begin by providing a concise overview of its implementation details and noteworthy technical challenges encountered during development (§ 6.1). Next, we delve into the experimental setup, outlining the datasets, monetary cost considerations, baselines, and performance metrics used in the evaluation (§ 6.2). We then present a proof-of-concept demonstration for the paper’s core proposition: *the efficient and effective resolution of lack of coverage for under-represented groups* (§ 6.3). This demonstration serves as a foundational validation of the system’s functionality.

Finally, we conduct a comprehensive performance evaluation of individual design decisions and system components across three distinct tasks. Each task leverages a specific benchmark, and we present comparative analyses against state-of-the-art baselines to objectively assess the system’s effectiveness.

- ① We investigate the system’s performance in passing the data distribution test (§ 3.1) and quality evaluation test (§ 3.2), using various mask delineation levels and guide tuple strategies.
- ② We analyze the performance of the proposed GREEDY approach (Algorithm 1) for combinations selection.
- ③ Our quality evaluation test (§ 3.2) involves human evaluators. In presence of automated tools that perform similar to human evaluators, this step could be automated. In this experiment, we explore alternative options to replace human evaluators. We analyze the results obtained from different quality assessment tools and compare them to the ground truth by human evaluators.

6.1 Implementation Details

Architectural style. The implementation of CHAMELEON is based on a microservices architecture, providing modularity and independence for each project component. Employing microservices allows us to develop each aspect of the project as an independent service, communicating through APIs. It also gives us the ability to replace each service without interrupting others if required. All backend microservices are implemented using the FASTAPI framework, while the frontend service is developed using REACT JS. The various services in our project include Gateway, ImageAnalyzer, ImageEditor, MaskGenerator, PreProcessor, LinUCB, and Chameleon-UI.

Integration with Foundation Model. For seamless integration with DALL-E 2, specific formatting of input and output image sizes is imperative. All input images are required to be converted into square images with dimensions of 256x256, 512x512, or 1024x1024. To meet this criterion, we employ two distinct strategies. 1) *Cropping*: when dealing with data sets consisting images characterized by varying dimensions (portrait and landscape), we filter out images with a ratio of the larger side to the smaller side exceeding 1.5. This filtering ensures the keeping of predominantly square images in our data set. Subsequently, we perform a center crop and resize of all images to the nearest acceptable square size. 2) *Encasing*: in instances where all images share uniform dimensions and exhibit elongated rectangular shapes, direct cropping may result in the loss of important features. To address this, we encase each image within a larger square image with a white background. Post DALL-E 2 image generation, we transform the resulting tuple to match the dimensions of the original data set, effectively removing the surplus white area.

6.2 Experimental Setup

6.2.1 Hardware Configurations. The majority of the development and testing for CHAMELEON occurred on a personal computer equipped with 12 x86 cores and 16 gigabytes of memory. For experiments that required training a CNN model, we utilized an UBUNTU Linux server featuring 24 x86 cores and 128 gigabytes of memory.

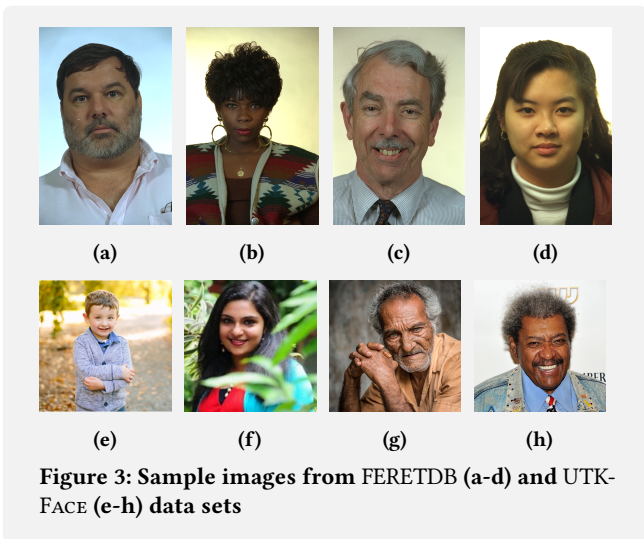


Figure 3: Sample images from FERETDB (a-d) and UTKFACE (e-h) data sets

6.2.2 Data Sets. We utilize distinct subsets from UTKFACE [75] and FERETDB [54] in our experiments. UTKFACE encompasses over 20,000 face images with annotation of age, gender, and ethnicity. The images in UTKFACE cover large variation in pose, facial expression, illumination, occlusion, resolution, and other factors. Conversely, FERETDB comprises 1199 individual images and serves as a standardized facial image database for researchers to develop algorithms and report results. All images in FERETDB share the same dimensions, pose, and facial expression and are annotated with gender and ethnicity. Figure 3 presents actual samples from both data sets.

6.2.3 Foundation Model and the Monetary Cost. We use DALL-E 2 Foundation model for generating images from prompt as it is (at the time of experiments) the most widely available Image Generation model with public API KEY available. Throughout the development and experimental phases, a total of 1962 distinct images were generated using DALL-E 2. *The total cost for generating these images amounted to (US)\$33.6.*

6.2.4 Evaluated Algorithms and Baselines. The following are the baselines and evaluated algorithms designed for each task.

- For Task ①, we consider NO-GUIDE TUPLE, along with SIMILAR-TUPLE and RANDOM-GUIDE strategies, as baselines for our experiments to compare against LINUCB. Additionally, we consider ACCURATE, MODERATE, and IMPRECISE mask delineation levels for evaluation.
- For Task ②, we consider two baselines to compare against the GREEDY combination selection algorithm. The first baseline, called RANDOM, randomly selects the next combination to be generated. The second baseline (MIN-GAP), however, first identifies a MUP M that requires the minimum number of instances to be covered. It then generates a combination that matches M . Both RANDOM and MIN-GAP baselines continue until the MUPs at smallest level are resolved.
- For Task ③, we employ state-of-the-art image quality assessment tools, NIMA [69], BRISQUE [46] and NIQE [47] as baselines for comparing results with human ground truth.

Table 2: Demographic groups distribution in FERETDB

	Male	Female	Total
White	331	229	560
Black	21	19	40
Asian	80	47	127
Hispanic	11	8	19
Middle Eastern	9	1	10
Total	452	304	756

- Lastly, for our proof of concept, we designate the TENSORFLOW KERAS CNN Model for precision, recall and F1 score comparisons.

6.2.5 *Performance metrics.* In Task ①, our performance metrics include the Quality Test Acceptance Rate and Data Distribution Test Acceptance Rate of the generated samples. For Tasks ②, our primary performance metric is the number of queries incurred by \mathcal{F} , representing the cost of image generation. In Task ③, our evaluation metrics are the Jaccard similarity of each algorithm’s output with the ground truth. Finally, in our proof of concept, our metric focuses on the precision, recall and F1 score of the trained model on the test data set.

6.3 Proof of Concept

Our approach for resolving lack of coverage issues in a multi-modal data set is by augmenting it with *synthetically generated data*. We start our experiments by investigating the *feasibility*, *effectiveness*, and *efficiency* of this data-repair approach.

To do so, we illustrate the impact of lack of coverage resolution using CHAMELEON in a down-stream machine learning task. We start by measuring the unfairness (in form of performance disparity) of a model trained on the original data set for under-represented groups. Next, we repair the data set, using CHAMELEON, and repeat the process to see if the unfairness issues reduce. Subsequently, we monitor the so-called “price of fairness”, i.e., the reduction in the overall performance as a result of unfairness reduction (data repair).

Our experiment employs the entire FERETDB data set as input, with detailed demographic group counts provided in Table 2. While the data set has a reasonable coverage for both male and female genders, the racial groups Black, Hispanic, and Middle eastern are not covered (using the coverage threshold $\tau = 100$). We trained a race-predicting Convolutional Neural Network (CNN) model using this data set. First, we observed an high overall performance of the model, with precision, recall, and F1-score being, 0.81, 0.75, and 0.78, respectively. Moreover, the model shows similar performance on both (covered) genders. However, as reflected in Table 3 (the “classifier performance on FERETDB” column), the model significantly under-performs for the uncovered groups. For example, while the overall F1-score is 78%, it is as low as 16%, 25%, and 0%, for the Black, Hispanic, and Middle eastern groups, respectively.

To evaluate if resolving the lack of coverage for these groups using CHAMELEON helps to reduce the gaps, we employ it with the GREEDY combination selection algorithm, Moderate mask delineation level, and the LINUCB approach, to resolve the level-1 MUPs, i.e., the three uncovered racial groups. In total, CHAMELEON issued

307 queries to the foundation model, of which 231 pass both the quality and distribution tests. That is, 75% of the generated images passed the rejection sampling tests. We refer to the augmented data set as “Repaired”. Utilizing DALL·E 2 to generate 307 images incurred a total cost of \$4.91 (\$0.016 per image).

Next, we retrain the CNN using the Repaired data set. Notably, the test data remains the same for both experiments and only contains real images. First, as expected, from Table 3 (the “classifier performance on Repaired” column), one can notice a slight decrease on the overall performance of the model as a result of data augmentation. On the other hand though, it is evident that *the performance of the model significantly increased for all under-represented groups, across all performance metrics*. For example, looking at the F1-scores, the performance improvement was more than 20% in all cases.

Figures 4a, 4b, and 4c show the model unfairness in form of Disparate Performance (F1-Disparity, Precision-Disparity, and Recall-Disparity) across the under-represented groups in the FERETDB data set, before and after the data repair. The performance disparity for an under-represented group is computed as its performance ratio gap with the overall model performance. For example, if the overall performance of the model for a metric p (e.g., F1-score) is ρ_{all} and for a group g is ρ_g , the unfairness is computed as

$$p\text{-Disparity}(g) = \max\left(0, 1 - \frac{\rho_g}{\rho_{all}}\right)$$

The figure demonstrates a clear reduction in disparities for all underrepresented groups after the repair process, which showcases the effectiveness of the data augmentation using CHAMELEON. For example, the F1-disparity for the Black group decreased from 79% to 27%.

Price of Fairness. Due to the trade-offs between the model performance and fairness, improving fairness is usually associated with a reduction in the overall model performance, which is known as the *price of fairness*. As we saw earlier, our data repair approach using CHAMELEON could significantly reduce the model performance disparities for the under-represented groups. This, however, comes at the cost of a slight model performance reduction. Figure 4 shows this cost, as the reduction in overall Precision, Recall, and F1-Score after data augmentation. The price of fairness, as reflected in various metrics, is modest compared to the substantial improvement in fairness achieved for under-represented groups.

6.4 Performance Evaluation

6.4.1 *Investigating the Influence of Mask Levels and Guide Image Selection on Quality Assessment* ①. This study explores the impact of different mask delineation levels and guide tuple selection strategies on the performance of generated tuples in passing rejection sampling tests. A total of 37 individuals participated as the human evaluators for the quality evaluation test.

To guarantee an inclusive evaluation, we intentionally constructed a challenging subset of the UTKFACE data set. This subset was designed to encompass Maximal Uncovered Patterns (MUPs) for all races and genders. Within each age group, we introduced two distinct ℓ_3 MUPs, each representing a different combination of gender and race (e.g., White male adult, Indian female adult). This approach ensures comprehensive coverage of various races, genders, and age

Table 3: Illustration of repairing lack of coverage and its effects on FERETDB

Ethnicity Groups	Classifier Performance on FERETDB				Classifier Performance on Repaired			
	#Images	Precision	Recall	F1-Score	#Images	Precision	Recall	F1-Score
Overall	756	0.81	0.75	0.78	987	0.70	0.75	0.72
Black	40	0.19	0.22	0.16	100	0.48	0.56	0.52
Hispanic	19	0.50	0.17	0.25	100	0.62	0.36	0.45
Middle Eastern	10	0.00	0.00	0.00	100	0.20	0.41	0.27

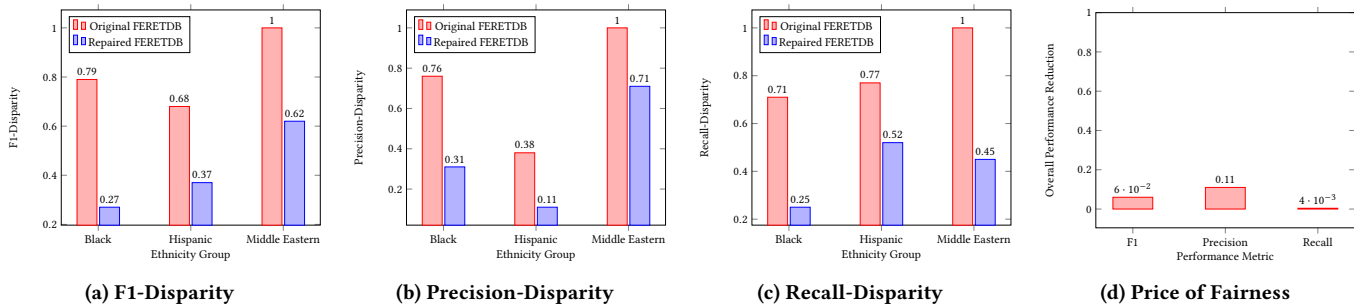


Figure 4: Unfairness (disparate performance) reduction for the uncovered groups in the FERETDB data set after data repair using CHAMELEON, along with the price of fairness (overall performance reduction).

Table 4: Performance of various Guide-selection algorithms

Guide Tuple Strategy	Mask Delineation Level	Quality Test Acceptance Rate		Data Distribution Test Acceptance Rate ($\nu = 0.3$)	
		$\alpha = 0.1$	$\alpha = 0.4$	Linear	RBF
		No Guide	-	0.90	0.81
Random-Guide	Accurate	0.69	0.51	0.70	0.74
	Moderate	0.85	0.70	0.70	0.70
	Imprecise	0.90	0.70	0.73	0.62
	Avg:	0.81	0.64	0.71	0.69
Similar-Tuple	Accurate	0.88	0.69	0.65	0.67
	Moderate	0.90	0.75	0.64	0.58
	Imprecise	0.85	0.68	0.65	0.53
	Avg:	0.88	0.71	0.65	0.59
LinUCB	Accurate	0.90	0.81	0.63	0.61
	Moderate	0.91	0.88	0.64	0.58
	Imprecise	0.96	0.96	0.63	0.54
	Avg:	<u>0.92</u>	<u>0.88</u>	0.63	0.58

groups during image generation. The exclusive use of ℓ_3 MUPs guarantees that all experiments will generate identical combinations, effectively eliminating any potential randomness or variability in the results.

In total, we introduced 16 MUPs within the UTKFACE subset with $\tau = 10$. Our objective was to resolve all MUPs in the subset for all possible combinations of guide tuple selection strategies and mask delineation levels. We then compared the Quality Test Acceptance Rate (QTAR) and Data Distribution Test Acceptance Rate (DDTAR) for each combination.

We generated a total of 831 images for these experiments and employed 27 human evaluators to assess their quality. Each evaluator received 200 images, presented in 8 pages of 25 images each. They

were instructed to identify images that appear *unrealistic* to human beings. A sample of the evaluation form presented to participants is provided in Figure 5.

In a separate experiment, we employed 10 human evaluators for estimating the probability p (Equation 1) that an evaluator labels a real image as realistic. To do so, we used the same forms as in Figure 5, except that this time all images were real, from the original data set. For UTKFACE, the probability p was estimated as 0.86.

For each setting, the Quality Test Acceptance Rate (QTAR) is defined as the number of images passing the quality test (§ 3.2) divided by the total number of generated images. To explore the impact of evaluation stringency on QTAR, we calculated it for two significance levels, $\alpha = 0.1$ and $\alpha = 0.4$. A higher α value signifies a

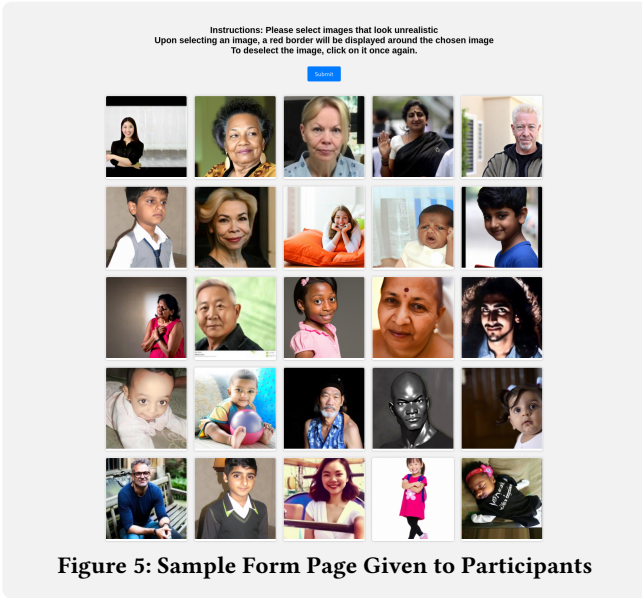


Figure 5: Sample Form Page Given to Participants

stricter acceptance policy, demanding a greater agreement among evaluators regarding image looking realistic.

For $\alpha = 0.4$, acceptance closely aligns with *unanimous agreement* among evaluators, whereas $\alpha = 0.1$ approximates a *majority vote*, accepting images deemed realistic by over half of the evaluators. This distinction results in a trade-off between quality and quantity, with $\alpha = 0.4$ yielding a smaller pool of images passing the test, with potentially higher overall quality. Table 4 presents the calculated QTAR values for the designed UTKFACE subset under both significance levels.

The analysis of Quality Test Acceptance Rate (QTAR) reveals that the LINUCB guide tuple selection strategy consistently outperforms No Guide, Similar-Tuple, and Random-Guide across both significance levels ($\alpha = 0.1$ and $\alpha = 0.4$). This performance gap widens further as the quality assessment becomes stricter (higher α). Notably, images generated using LINUCB exhibit demonstrably higher overall quality.

Further investigation into the interplay between guide-tuple selection strategies and mask delineation levels uncovers interesting trends. For both significance levels, Moderate and Imprecise mask delineation levels achieve superior QTAR compared to the Accurate level. This finding aligns with our initial expectations. Precisely cropping the foreground subject restricts the Foundation Model’s creative freedom, potentially leading to unnatural entities generated to fill the cropped space. Conversely, Moderate and Imprecise levels provide greater flexibility, allowing the Foundation Model to generate new objects more naturally and potentially contributing to improved image quality.

Next, we move to the data distribution test (§ 3.1). DDTAR, defined as the proportion of images passing the test, assesses how well the generated images adhere to the underlying data distribution. We use MOBILENETV3[33] as the embedder and OCSVM ($\nu = 0.3$) with two kernels (RBF and Linear) for training. The choice of the kernel impacts the performance of the OCSVM, with the RBF kernel

often capturing complex relationships in the data, while the Linear kernel assumes linearity.

The No-Guide strategy does not provide a guide for the image generation process, leaving the details to the imagination of the foundation model. As a result, it is anticipated that a larger portion of the images generated with this strategy should fail the data distribution test. This is confirmed in Table 4, where around half of the images generated with this strategy (using either of the two kernels) could not pass the test. On the other hand, the Random-Guide strategy is focused on following the data distribution. Therefore, viewing the images in the data set as the random iid samples from its underlying distribution, it draws a random image from the data set and uses it as the guide, irrespective of the description of the image to be generated. This approach, while has a smaller chance of passing the quality test, is expected to have the highest chance of passing the data distribution test. Our findings in Table 4 are consistent with this expectation. While the Random-Guide strategy outperforms LINUCB and the Similar-Tuple strategy on the data distribution test, both of these strategies still demonstrate acceptable performance. Regarding mask delineation levels, Accurate delineation exhibits marginally higher DDTAR compared to Moderate and Imprecise levels. This aligns with our expectations, as stricter cropping likely helps constrain the generated images to closer proximity to the original data distribution. However, the performance difference is relatively small, suggesting that the advantages of Moderate and Imprecise delineation in terms of naturalness and flexibility outweighs the slight decrease in distribution adherence for tight boundaries.

Overall, since LINUCB *outperforms the other approaches on the quality evaluation test (which involves human evaluators) and shows an acceptable performance on the data distribution test*, it is the preferred approach for guide-selection.

6.4.2 GREEDY Combination Selection Algorithm ②. In this experiment, we study the impact of employing the GREEDY algorithm for selecting the next combination to generate tuples. The entire UTKFACE data set serves as input for our investigation, where we analyze the cost of repairing all ℓ_1 or ℓ_2 MUPs for different thresholds using various combination selection algorithms. As a baseline, we employ the Random selection algorithm, which randomly chooses a combination in each iteration without considering the MUPs’ status. We also introduce the MIN-GAP algorithm, which given list of MUPs, first identifies the MUP which has smallest gap δ from threshold τ , then chooses a combination that satisfies this MUP and generates δ tuples to satisfy that MUP. Unlike the GREEDY algorithm, the MIN-GAP Algorithm only focuses on the distance from the threshold, disregarding the number of MUPs hit and MUPs level. We conduct experiments with four distinct values for τ and monitor the total number of images each algorithm requires to add to the data set for resolving the MUPs.

For $\tau = 200$ and $\tau = 350$, all MUPs are at levels ℓ_2 and ℓ_3 . In these experiments we the goal is to resolve ℓ_2 MUPs. For $\tau = 1000$ and $\tau = 2000$, where ℓ_1 , ℓ_2 , and ℓ_3 MUPs are present, our focus is on resolving all ℓ_1 MUPs.

Figure 6 shows the associated cost (total number of images to be generated) for each strategy in different scenarios. We can observe that in all cases GREEDY algorithm significantly outperforms both

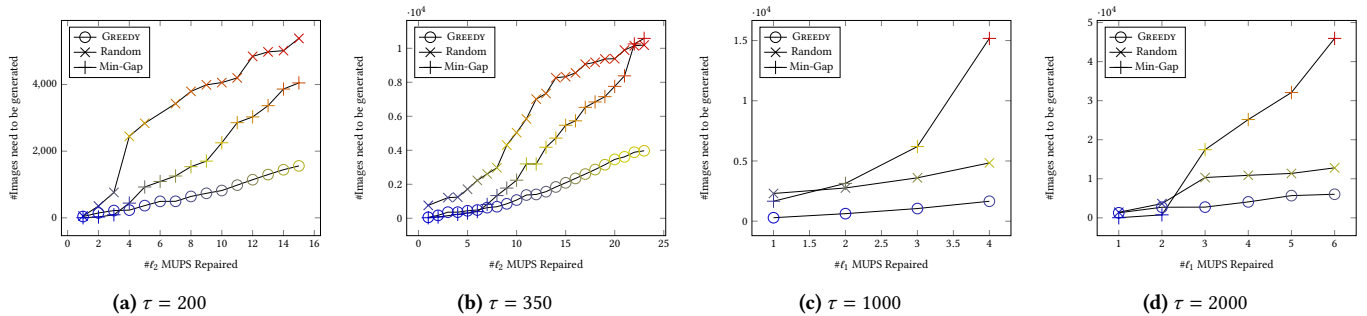


Figure 6: Comparison of cost across various thresholds for GREEDY, Random, and Min-Gap combination selection algorithms

Table 5: Jaccard similarity of the output of each image quality assessment algorithm with the ground truth set

Quality Assessment Algorithm	J_s
NIQE	0.127
BRISQUE	0.068
NIMA	0.068

Random and MIN-GAP baselines. The Gap even becomes more noticeable when trying to resolve lower level MUPs. In addition, the MIN-GAP strategy performs better than Random for ℓ_2 MUPs but significantly worse when attempting to satisfy the ℓ_1 MUPs. This is due to the larger pool of MUPs in higher thresholds, as the Min-Gap algorithm may choose numerous irrelevant MUPs to satisfy, leaving ℓ_1 MUPs unsatisfied for subsequent iterations.

6.4.3 Quality Assessment Tools Comparison ③. In this experiment we investigate the performance of multiple image quality assessment algorithms by comparing their outputs with human evaluator ground truth. The objective is to explore the feasibility of transitioning from human evaluators to automated tools. Before continuing, we would like to underscore that the purpose of this step is not similar to “fake image” detectors, such as in [36, 43], to distinguish between synthesized and authentic images. Note that, the evaluated images in this step are indeed machine-generated.

Image quality evaluation can be accomplished using established techniques such as Blind/Referenceless Image Spatial Quality Evaluator (BRISQUE) [46], Neural Image Assessment (NIMA) [69], or Natural Image Quality Evaluator (NIQE) [47]. For instance, given an image to evaluate, NIQE first generates a masked version of the image using the weighted local mean and contrast of the image in the vicinity of each pixel. It then creates a feature matrix for the image using a Multivariate Gaussian (MVG) density model. The mean and covariance of the feature matrix (compared with those of a training set) are then used to assign a quality measure and classifying the image as “good quality” or not. Each algorithm returns a score, and an acceptance threshold τ_c is defined for each tool. We fine-tune τ_c based on the actual number of rejected images.

In this experiment, a dataset of 271 synthetic images, generated using guide images from UTKFACE and varying mask delineation levels is subjected to 7 human evaluators. Each evaluator is asked

to identify images that “do not look realistic.” with an average exposure of each image to more than five evaluators. We use labeling procedure outlined in § 3.2 with significance level $\alpha = 0.1$ to label images. Out of the total, 27 images are marked as “unacceptable” while the remaining images are labeled as acceptable.

We subjected the ground truth dataset to BRISQUE [46], NIMA [69] and NIQE [47]. For each algorithm, we calibrated acceptance thresholds to reject precisely 27 images, aligning with the number identified as unacceptable by human evaluators. We compared the sets of rejected images between each algorithm and the ground truth using Jaccard Similarity. This metric quantifies the degree of overlap between the sets, with values closer to 1 indicating stronger agreement. Table 5 presents the Jaccard Similarity scores for each algorithm. Results reveal that none of the assessed algorithms achieved satisfactory performance in reliably isolating unrealistic images.

7 RELATED WORK

While data bias has been a long-standing concern in the statistical community [52], social data presents unique challenges due to its inherent complexity and sensitivity [8, 9, 26, 37, 53]. Issues of diversity and representativeness have been studied across various disciplines, including social science [10, 25, 66], political science [67], and information retrieval [3]. Efforts to trace machine bias back to its sources involve identifying different types [30, 45, 53] and sources [22, 24, 70] of biases in data. Existing work to meet *responsible data* requirements [51] extend throughout various stages of the data analysis pipeline, including data annotation [39, 41], data cleaning and repair [57, 58, 68], data imputation [44], entity resolution [28, 61], and data integration [50, 51].

Data Coverage. The notion of data coverage has been proposed for detecting under-representation issues in a data set [62]. Related work in this area can be divided into (a) lack of coverage detection and (b) lack of coverage resolution. Coverage detection in tabular data has been studied for both discrete [5] and continuous [6] attributes, whether in single or multiple relations [42], and recently for image data set [48]. Efforts for addressing lack of coverage without additional data collection include query rewriting [1, 2, 64] and generating lack of representation warning [60]. On the other hand, data tailoring [50] has been proposed to integrate additional data from a data lake to resolve under-representation issues. Differently, for tabular data, [17, 34, 63] partially alter duplicates of existing tuples, or generate synthetic entries from existing data to resolve

lack of coverage. For a comprehensive survey on representation bias in data, refer to [62].

Foundation Models for Data Management. With recent advancements in large language models [13, 23, 71] and foundation models, those have been widely used in various research communities for tasks such as Code Generation [20], Synthetic Image Generation [55], and Video Generation [7]. The current state of utilizing these models in the data management community reflects a growing recognition of their potential and challenges. Some of the recent work within for utilizing generative AI for data management problems are as following. LLMs have shown an extraordinary performance for answering natural language queries [18, 73, 74]. Particularly, THALAMUSDB enables answering complex natural language queries on multi-modal data [35]. LLMs and foundation models have also been utilized for challenging tasks such as data set search [73], predicting data correlations [72], data-lake profiling [4], and anomaly detection in time-series [21], to name a few. Still, to the best of our knowledge, none of the existing work has utilized foundation models for fairness-aware multi-modal data augmentation.

8 PROOFS

LEMMA 1. COMBINATION-SELECTION is NP-hard.

Proof: We prove the NP-hardness of COMBINATION-SELECTION using the reduction from *Vertex-cover* (VC). In the proof, we assume the combinations C to choose from are specified as part of the input to COMBINATION-SELECTION.

The input to VC is $G(V, E)$, a graph with the set of vertices $V = \{v_1, \dots, v_{n'}\}$ and the set of edges $E = \{e_1, \dots, e_{m'}\}$. Then, given a value k , the decision version of VC determines if there exists a subset $V' \subseteq V$ of size (at most) k , such that all edges are covered, i.e., $\forall e_i = (u, v) \in E, \{u, v\} \cap V' \neq \emptyset$.

Given a target value k , the decision version of COMBINATION-SELECTION problem determines if there exists an assignment to σ -values such that $\sum_{C_i \in C} \sigma_i \leq k$, while all MUPs $M \in \mathcal{M}^*$ are resolved. Given an instance of VC, we reduce it to COMBINATION-SELECTION in P -time as following:

- For each edge e_i , add a binary attribute x_i to the attributes of interest. That is $\mathbf{x} = \{e_1, \dots, e_{n'}\}$.
- Consider the binary matrix C , with m' rows and the columns e_1 to $e_{n'}$. Add m' rows v_1 to $v_{m'}$, where the i -th row corresponds with the vector v_i . For each edge $e_i = (v_j, v_k)$, set the cells $C_{i,j}$ and $C_{i,k}$ as 1 and all other cells in column e_i as 0. Therefore, in sum of the values on each column is exactly 2. The rows of matrix C represent the combinations to choose from. In other words, for each vector $v_i \in V$, a binary value combination C_i is added, where (only) the cells corresponding to its edges are one.
- For each edge e_i add the level-1 MUP $M_i = X \cdot \dots \cdot X1X \cdot \dots$, where the i -th element is 1 and all others are unspecified. Set $\delta(M_i) = 1$.
- Set the target value in the decision version of COMBINATION-SELECTION as k .

Now, the output to the VC problem is yes, i.e., a vertex cover of size at most k exists, if and only if the output to the COMBINATION-SELECTION problem is yes. As a result, since VC is NP-complete, COMBINATION-SELECTION is NP-hard, unless P=NP. \square

THEOREM 1. The approximation ratio of the GREEDY approach is $\log(\eta)$, where $\eta = \sum_{M \in \mathcal{M}^*} \delta(M)$.

Proof: At every iteration, the GREEDY algorithm selects a combination that contributes the most in reducing the coverage gap for a subset of remaining MUPs in \mathcal{M}^* . In order to prove the approximation ratio, we assign a price of 1 for each time a combination c is selected, i.e., for each increase of 1 in the count of $\sigma(c)$. This price is uniformly distributed across the remaining MUPs that c match to. Now, let us define the variable $e[i, j]$ that shows the price paid by the algorithm to reduce the gap of M_i for the j -th time (each time the gap is reduced by one). For example, if during the current iteration, the selected combination c matches the remaining MUPs $\{M_2, M_5, M_7\}$, while this is the first match for M_2 , the 6-th match for M_5 , and the second match for M_7 , we set $e[2, 1] = 1/3$, $e[5, 6] = 1/3$, and $e[7, 3] = 1/3$.

Let us consider the ordering of $e[i, j]$ values from the smallest to largest and let $\eta = \sum_{M \in \mathcal{M}^*} \delta(M)$. Let the ordered list be indexed as $\mathbf{e} = \langle e_1, e_2, \dots, e_\eta \rangle$.

Now, let OPT be the total sum of the optimal combination-counts (i.e., $\min \sum \sigma_i$) for resolving the MUPs \mathcal{M}^* . In other words, OPT is the total price that the optimal algorithm pays to fills the gaps for all MUPs in \mathcal{M}^* . For each $e_i = e[k, j]$ in the ordered list, let e_i^o be the price assigned to match M_k for the j -th time. Uniformly distributing OPT across $\langle e_i, e_{i+1}, \dots, e_\eta \rangle$, we know that

$$e_i^o \leq \frac{OPT}{\eta - i + 1}$$

Also, since at each iteration, greedy selects the combination that matches the maximum number of remaining MUPs

$$e_i \leq e_i^o$$

Let A be the total sum of the combination-counts by the GREEDY algorithm. Since A is distributed between the elements of \mathbf{e} ,

$$A = \sum_{i=1}^{\eta} e_i \leq \sum_{i=1}^{\eta} e_i^o \leq \sum_{i=1}^{\eta} \frac{OPT}{\eta - i + 1} = OPT \sum_{i=1}^{\eta} \frac{1}{\eta - i + 1}$$

$$\sum_{i=1}^{\eta} \frac{1}{\eta - i + 1} = \sum_{i=1}^{\eta} \frac{1}{i} = H_\eta$$

$$\Rightarrow A \leq OPT H_\eta = OPT \Theta(\log(\eta))$$

$$\Rightarrow \frac{A}{OPT} \leq \Theta(\log(\eta))$$

\square

9 CONCLUSION

In this paper, we introduced CHAMELEON for fairness-aware data augmentation to reduce the under-representation of minority groups. Motivated by the recent advancements in the foundation models, our system efficiently utilizes them for data-repair with minimum addition of synthetically generated data, while ensuring the augmented data is of high quality and follows the underlying data distribution. Our experiment results demonstrated the effectiveness of our data-repair approach in reducing the unfairness of a downstream task. This motivates the future work to extend the scope of fairness-aware data augmentation to other settings such as natural language data and graph data, using large language models.

REFERENCES

- [1] Chiara Accinelli, Barbara Catania, Giovanna Guerrini, and Simone Minisi. 2021. The impact of rewriting on coverage constraint satisfaction. In *EDBT Workshops*.
- [2] Chiara Accinelli, Simone Minisi, and Barbara Catania. 2020. Coverage-based Rewriting for Data Preparation. In *EDBT Workshops*.
- [3] Rakesh Agrawal, Sreenivas Gollapudi, Alan Halverson, and Samuel Ieong. 2009. Diversifying search results. In *WSDM*. ACM, 5–14.
- [4] Simran Arora, Brandon Yang, Sabri Eyuboglu, Avnika Narayan, Andrew Hojel, Immanuel Trummer, and Christopher Ré. 2023. Language Models Enable Simple Systems for Generating Structured Views of Heterogeneous Data Lakes. *PVLDB* 17, 2 (2023), 97–105.
- [5] Abolfazl Asudeh, Zhongjun Jin, and HV Jagadish. 2019. Assessing and remedying coverage for a given dataset. In *2019 IEEE 35th International Conference on Data Engineering (ICDE)*. IEEE, 554–565.
- [6] Abolfazl Asudeh, Nima Shahbazi, Zhongjun Jin, and H. V. Jagadish. 2021. Identifying Insufficient Data Coverage for Ordinal Continuous-Valued Attributes. In *SIGMOD*. ACM.
- [7] Omer Bar-Tal, Hila Chefer, Omer Tov, Charles Herrmann, Roni Paiss, Shiran Zada, Ariel Ephrat, Junhwa Hur, Yuanzhen Li, Tomer Michaeli, et al. 2024. Lumiere: A Space-Time Diffusion Model for Video Generation. *arXiv preprint arXiv:2401.12945* (2024).
- [8] Solon Barocas, Moritz Hardt, and Arvind Narayanan. 2019. Fairness and machine learning: Limitations and opportunities. fairmlbook.org.
- [9] Solon Barocas and Andrew D Selbst. 2016. Big data’s disparate impact. *Calif. L. Rev.* 104 (2016), 671.
- [10] Ellen Berrey. 2015. *The enigma of diversity: The language of race and the limits of racial justice*. University of Chicago Press.
- [11] Rishi Bommasani, Drew A Hudson, Ehsan Adeli, Russ Altman, Simran Arora, Sydney von Arx, Michael S Bernstein, Jeannette Bohg, Antoine Bosselut, Emma Brunskill, et al. 2021. On the opportunities and risks of foundation models. *arXiv preprint arXiv:2108.07258* (2021).
- [12] Djallel Bouneffouf, Irina Rish, and Charu Aggarwal. 2020. Survey on applications of multi-armed and contextual bandits. In *2020 IEEE Congress on Evolutionary Computation (CEC)*. IEEE, 1–8.
- [13] Tom Brown, Benjamin Mann, Nick Ryder, Melanie Subbiah, Jared D Kaplan, Prafulla Dhariwal, Arvind Neelakantan, Pranav Shyam, Girish Sastry, Amanda Askell, et al. 2020. Language models are few-shot learners. *Advances in neural information processing systems* 33 (2020), 1877–1901.
- [14] Sébastien Bubeck, Varun Chandrasekaran, Ronen Eldan, Johannes Gehrke, Eric Horvitz, Ece Kamar, Peter Lee, Yin Tat Lee, Yuanzhi Li, Scott Lundberg, et al. 2023. Sparks of artificial general intelligence: Early experiments with gpt-4. *arXiv preprint arXiv:2303.12712* (2023).
- [15] Joy Buolamwini and Timnit Gebru. 2018. Gender shades: Intersectional accuracy disparities in commercial gender classification. In *Conference on fairness, accountability and transparency*. PMLR, 77–91.
- [16] Kuntai Cai, Xiaokui Xiao, and Graham Cormode. 2023. Privlava: synthesizing relational data with foreign keys under differential privacy. *Proceedings of the ACM on Management of Data* 1, 2 (2023), 1–25.
- [17] L Elisa Celis, Vijay Keswani, and Nisheeth Vishnoi. 2020. Data preprocessing to mitigate bias: A maximum entropy based approach. In *ICML*. PMLR, 1349–1359.
- [18] Shuaichen Chang and Eric Fosler-Lussier. 2023. How to Prompt LLMs for Text-to-SQL: A Study in Zero-shot, Single-domain, and Cross-domain Settings. *arXiv preprint arXiv:2305.11853* (2023).
- [19] Nitesh V. Chawla, Kevin W. Bowyer, Lawrence O. Hall, and W. Philip Kegelmeyer. 2002. SMOTE: Synthetic Minority Over-sampling Technique. *J. Artif. Intell. Res.* 16 (2002), 321–357. <https://doi.org/10.1613/jair.953>
- [20] Mark Chen, Jerry Tworek, Heewoo Jun, Qiming Yuan, Henrique Ponde de Oliveira Pinto, Jared Kaplan, Harri Edwards, Yuri Burda, Nicholas Joseph, Greg Brockman, et al. 2021. Evaluating large language models trained on code. *arXiv preprint arXiv:2107.03374* (2021).
- [21] Yuhang Chen, Chaoyun Zhang, Minghua Ma, Yudong Liu, Ruomeng Ding, Bowen Li, Shilin He, Saravan Rajmohan, Qingwei Lin, and Dongmei Zhang. 2023. ImDiffusion: Imputed Diffusion Models for Multivariate Time Series Anomaly Detection. *Proceedings of the VLDB Endowment* 17, 3 (2023), 359–372.
- [22] Kate Crawford. 2013. The hidden biases in big data. *Harvard business review* 1, 4 (2013).
- [23] Jacob Devlin, Ming-Wei Chang, Kenton Lee, and Kristina Toutanova. 2018. Bert: Pre-training of deep bidirectional transformers for language understanding. *arXiv preprint arXiv:1810.04805* (2018).
- [24] Nicholas Diakopoulos. 2015. Algorithmic accountability: Journalistic investigation of computational power structures. *Digital journalism* 3, 3 (2015), 398–415.
- [25] Frank Dobbin and Alexandra Kalev. 2016. Why diversity programs fail and what works better. *Harvard Business Review* 94, 7-8 (2016), 52–60.
- [26] Marina Drosou, HV Jagadish, Evangelia Pitoura, and Julia Stoyanovich. 2017. Diversity in big data: A review. *Big data* 5, 2 (2017), 73–84.
- [27] Ju Fan, Tongyu Liu, Guoliang Li, Junyong Chen, Yuwei Shen, and Xiaoyong Du. 2020. Relational data synthesis using generative adversarial networks: A design space exploration. *arXiv preprint arXiv:2008.12763* (2020).
- [28] Nikolaos Fanourakis, Christos Kontousias, Vasilis Efthymiou, Vassilis Christophides, and Dimitris Plexousakis. 2023. FairER demo: Fairness-Aware and Explainable Entity Resolution. (2023).
- [29] Bernard D Flury. 1990. Acceptance–rejection sampling made easy. *Siam Review* 32, 3 (1990), 474–476.
- [30] Batya Friedman and Helen Nissenbaum. 1996. Bias in computer systems. *TOIS* 14, 3 (1996), 330–347.
- [31] John Hammersley. 2013. *Monte carlo methods*. Springer Science & Business Media.
- [32] Hui Han, Wen-Yuan Wang, and Bing-Huan Mao. 2005. Borderline-SMOTE: a new over-sampling method in imbalanced data sets learning. In *Advances in Intelligent Computing: International Conference on Intelligent Computing, ICIC 2005, Hefei, China, August 23-26, 2005, Proceedings, Part I 1*. Springer, 878–887.
- [33] Andrew Howard, Mark Sandler, Grace Chu, Liang-Chieh Chen, Bo Chen, Mingxing Tan, Weijun Wang, Yukun Zhu, Ruoming Pang, Vijay Vasudevan, et al. 2019. Searching for mobilenetv3. In *Proceedings of the IEEE/CVF international conference on computer vision*. 1314–1324.
- [34] Vasileios Iosifidis and Eirini Ntoutsi. 2018. Dealing with bias via data augmentation in supervised learning scenarios. *Jo Bates Paul D. Clough Robert Jäschke* 24 (2018).
- [35] Saehan Jo and Immanuel Trummer. 2023. Demonstration of ThalamusDB: Answering Complex SQL Queries with Natural Language Predicates on Multi-Modal Data. In *Companion of the 2023 International Conference on Management of Data*. 179–182.
- [36] S Kiruthika and V Masilamani. 2023. Image quality assessment based fake face detection. *Multimed. Tools Appl* 82 (2023), 8691–8708.
- [37] Jon Kleinberg. 2019. Fairness, Rankings, and Behavioral Biases. *FAT**.
- [38] Jennifer Langston. 2015. Who’s a CEO? Google image results can shift gender biases. <https://www.washington.edu/news/2015/04/09/whos-a-ceo-google-image-results-can-shift-gender-biases/>.
- [39] Simone Lazier, Saravanan Thirumuruganathan, and Hadis Anahideh. 2023. Fairness and Bias in Truth Discovery Algorithms: An Experimental Analysis. *arXiv preprint arXiv:2304.12573* (2023).
- [40] Lihong Li, Wei Chu, John Langford, and Robert E Schapire. 2010. A contextual-bandit approach to personalized news article recommendation. In *Proceedings of the 19th international conference on World wide web*. 661–670.
- [41] Yanying Li, Haipei Sun, and Wendy Hui Wang. 2020. Towards fair truth discovery from biased crowdsourced answers. In *SIGKDD*. 599–607.
- [42] Yin Lin, Yifan Guan, Abolfazl Asudeh, and HV Jagadish. 2020. Identifying insufficient data coverage in databases with multiple relations. *Proceedings of the VLDB Endowment* 13, 12 (2020), 2229–2242.
- [43] Yun Liu, Zuliang Wan, Xiaohua Yin, Guanghui Yue, Aiping Tan, and Zhi Zheng. 2023. Detection of GAN generated image using color gradient representation. *Journal of Visual Communication and Image Representation* (2023), 103876.
- [44] Fernando Martínez-Plumed, César Ferri, David Nieves, and José Hernández-Orallo. 2019. Fairness and missing values. *arXiv preprint arXiv:1905.12728* (2019).
- [45] Ninareh Mehrabi, Fred Morstatter, Nripsuta Saxena, Kristina Lerman, and Aram Galstyan. 2021. A survey on bias and fairness in machine learning. *ACM Computing Surveys (CSUR)* 54, 6 (2021), 1–35.
- [46] Anish Mittal, Anush Krishna Moorthy, and Alan Conrad Bovik. 2012. No-reference image quality assessment in the spatial domain. *IEEE Transactions on image processing* 21, 12 (2012), 4695–4708.
- [47] Anish Mittal, Rajiv Soundararajan, and Alan C Bovik. 2012. Making a “completely blind” image quality analyzer. *IEEE Signal processing letters* 20, 3 (2012), 209–212.
- [48] Melika Mousavi, Nima Shahbazi, and Abolfazl Asudeh. 2024. Data Coverage for Detecting Representation Bias in Image Datasets: A Crowdsourcing Approach. In *EDBT*. 47–60.
- [49] M. Mulshine. 2015. A major flaw in Google’s algorithm allegedly tagged two black people’s faces with the word ‘gorillas’. *Business Insider*.
- [50] Fatemeh Nargesian, Abolfazl Asudeh, and HV Jagadish. 2021. Tailoring data source distributions for fairness-aware data integration. *Proceedings of the VLDB Endowment* 14, 11 (2021), 2519–2532.
- [51] Fatemeh Nargesian, Abolfazl Asudeh, and H. V. Jagadish. 2022. Responsible Data Integration: Next-generation Challenges. *SIGMOD* (2022).
- [52] Jerzy Neyman and Egon Sharpe Pearson. 1936. Contributions to the theory of testing statistical hypotheses. *Statistical Research Memoirs* (1936).
- [53] Alexandra Olteanu, Carlos Castillo, Fernando Diaz, and Emre Kiciman. 2019. Social data: Biases, methodological pitfalls, and ethical boundaries. *Frontiers in Big Data* 2 (2019), 13.
- [54] P Jonathon Phillips, Harry Wechsler, Jeffery Huang, and Patrick J Rauss. 1998. The FERET database and evaluation procedure for face-recognition algorithms. *Image and vision computing* 16, 5 (1998), 295–306.
- [55] Aditya Ramesh, Prafulla Dhariwal, Alex Nichol, Casey Chu, and Mark Chen. 2022. Hierarchical text-conditional image generation with clip latents. *arXiv preprint arXiv:2204.06125* 1, 2 (2022), 3.
- [56] Adam Rose. 2010. Are Face-Detection Cameras Racist? *Time Business*.

- [57] Babak Salimi, Bill Howe, and Dan Suciu. 2020. Database repair meets algorithmic fairness. *ACM SIGMOD Record* 49, 1 (2020), 34–41.
- [58] Babak Salimi, Luke Rodriguez, Bill Howe, and Dan Suciu. 2019. Interventional Fairness: Causal Database Repair for Algorithmic Fairness. In *SIGMOD*. ACM, 793–810.
- [59] Bernhard Schölkopf, Robert C Williamson, Alex Smola, John Shawe-Taylor, and John Platt. 1999. Support vector method for novelty detection. *Advances in neural information processing systems* 12 (1999).
- [60] Nima Shahbazi and Abolfazl Asudeh. 2022. Data-centric Reliability Evaluation of Individual Predictions. *CoRR, abs/2204.07682* (2022).
- [61] Nima Shahbazi, Nikola Danevski, Fatemeh Nargesian, Abolfazl Asudeh, and Divesh Srivastava. 2023. Through the Fairness Lens: Experimental Analysis and Evaluation of Entity Matching. *Proceedings of the VLDB Endowment* 16, 11 (2023), 3279–3292.
- [62] Nima Shahbazi, Yin Lin, Abolfazl Asudeh, and HV Jagadish. 2023. Representation Bias in Data: A Survey on Identification and Resolution Techniques. *Comput. Surveys* (2023).
- [63] Shubham Sharma, Yunfeng Zhang, Jesús M Ríos Aliaga, Djallel Bouneffouf, Vinod Muthusamy, and Kush R Varshney. 2020. Data augmentation for discrimination prevention and bias disambiguation. In *AIES*. 358–364.
- [64] Suraj Shetiya, Ian P. Swift, Abolfazl Asudeh, and Gautam Das. 2022. Fairness-Aware Range Queries for Selecting Unbiased Data. In *ICDE*. IEEE.
- [65] Mallory Simon. 2009. HP looking into claim webcams can't see black people. CNN.
- [66] Edward H Simpson. 1949. Measurement of diversity. *Nature* 163, 4148 (1949).
- [67] James Surowiecki. 2005. *The wisdom of crowds*. Anchor.
- [68] Ki Hyun Tae, Yuji Roh, Young Hun Oh, Hyunsu Kim, and Steven Euijong Whang. 2019. Data cleaning for accurate, fair, and robust models: A big data-AI integration approach. In *DEEM workshop*. 1–4.
- [69] Hossein Talebi and Peyman Milanfar. 2018. NIMA: Neural image assessment. *IEEE transactions on image processing* 27, 8 (2018), 3998–4011.
- [70] Antonio Torralba and Alexei A Efros. 2011. Unbiased look at dataset bias. In *CVPR 2011*. IEEE, 1521–1528.
- [71] Hugo Touvron, Thibaut Lavril, Gautier Izacard, Xavier Martinet, Marie-Anne Lachaux, Timothée Lacroix, Baptiste Rozière, Naman Goyal, Eric Hambro, Faisal Azhar, et al. 2023. Llama: Open and efficient foundation language models. *arXiv preprint arXiv:2302.13971* (2023).
- [72] Immanuel Trummer. 2023. Can Large Language Models Predict Data Correlations from Column Names? *Proceedings of the VLDB Endowment* 16, 13 (2023), 4310–4323.
- [73] Immanuel Trummer. 2023. Demonstrating GPT-DB: Generating Query-Specific and Customizable Code for SQL Processing with GPT-4. *Proceedings of the VLDB Endowment* 16, 12 (2023), 4098–4101.
- [74] Yunhu Ye, Binyuan Hui, Min Yang, Binhua Li, Fei Huang, and Yongbin Li. 2023. Large language models are versatile decomposers: Decompose evidence and questions for table-based reasoning. *arXiv preprint arXiv:2301.13808* (2023).
- [75] Zhifei Zhang, Yang Song, and Hairong Qi. 2017. Age Progression/Regression by Conditional Adversarial Autoencoder. In *IEEE Conference on Computer Vision and Pattern Recognition (CVPR)*. IEEE.
- [76] Ce Zhou, Qian Li, Chen Li, Jun Yu, Yixin Liu, Guangjing Wang, Kai Zhang, Cheng Ji, Qiben Yan, Lifang He, et al. 2023. A comprehensive survey on pretrained foundation models: A history from bert to chatgpt. *arXiv preprint arXiv:2302.09419* (2023).